

2022

Analysis of Power Quality Issues of Different Types of Household Applications

T.M. Thamizh Thentral
SRM Institute of Science and Technology, India

R. Palanisamy
SRM Institute of Science and Technology, India

S. Usha
SRM Institute of Science and Technology, India

Follow this and additional works at: <https://arrow.tudublin.ie/engscheleart2>

 *next page for additional authors*
Part of the [Electrical and Computer Engineering Commons](#)

Recommended Citation

Thamizh Thentral, T.M., Palanisamy, R. & Usha, S. (2022). Analysis of Power Quality Issues of Different Types of Household Applications. *Energy Reports*, vol. 8, pg. 5370–5386. doi:10.1016/j.egy.2022.04.010h

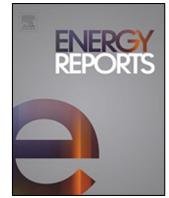
This Article is brought to you for free and open access by the School of Electrical and Electronic Engineering at ARROW@TU Dublin. It has been accepted for inclusion in Articles by an authorized administrator of ARROW@TU Dublin. For more information, please contact arrow.admin@tudublin.ie, aisling.coyne@tudublin.ie, gerard.connolly@tudublin.ie.



This work is licensed under a [Creative Commons Attribution-NonCommercial-Share Alike 4.0 License](#)
Funder: The European Union's Horizon 2020 research and Enterprise Ireland, Marie Skłodowska-Curie grant agreement No. 847402. National Research and Development Agency of Chile (ANID), ANID/Fondap/15110019.

Authors

T.M. Thamizh Thentral, R. Palanisamy, S. Usha, Mohit Bajaj, Hossam Zawbaa, and Salah Kamel



Research paper

Analysis of Power Quality issues of different types of household applications

T.M. Thamizh Thentral^a, R. Palanisamy^a, S. Usha^a, Mohit Bajaj^b, Hossam M. Zawbaa^{c,d,*}, Salah Kamel^e

^a Department of EEE, SRM institute of science and technology, Kattankulathur 603203, Chennai, India

^b Department of Electrical and Electronics Engineering, National Institute of Technology, New Delhi 110040, India

^c Faculty of Computers and Artificial Intelligence, Beni-Suef University, Beni-Suef, Egypt

^d Technological University Dublin, Dublin, Ireland

^e Department of Electrical Engineering, Faculty of Energy Engineering, Aswan University, Aswan 81528, Egypt

ARTICLE INFO

Article history:

Received 27 January 2022
Received in revised form 23 March 2022
Accepted 5 April 2022
Available online 22 April 2022

Keywords:

Power Quality issues
Total harmonics distortion
Different load combinations
Power factor
non-linear loads

ABSTRACT

Most of the loads used in our day-to-day life are non-linear in nature. To investigate the performance of various non-linear loads, a laboratory setup on different load combinations such as light, fan and drive system in this work. The unbalance in supply voltages, supply current and frequency, reduction in power factor and total harmonic distortion for current and voltages are monitored through this lab setup and also the results obtained from these systems are discussed in this paper. To check the nature of voltage, current, reactive power and power factor in real-time systems, a turret punch machine incorporated with several single-phase AC servo motors is considered. The variations in the parameters are recorded using the fluke analyzer. Finally, it is observed that current harmonics at the source side are dominant in both the laboratory setup and the real-time system. Next, shunt active power filters are applied to mitigate the current harmonics. The simulation for the system with compensations is conducted in the Matlab platform and the hardware implementation validates the same.

© 2022 The Author(s). Published by Elsevier Ltd. This is an open access article under the CC BY-NC-ND license (<http://creativecommons.org/licenses/by-nc-nd/4.0/>).

1. Introduction

Power Quality (PQ) issues are commonly categorized by a few terms to which any consumer may find such information farfetched when the topic taken goes deeper. Programmable logic controllers, Arc furnaces, welding machines, variable speed drives and digital storage devices like computers used in most industrial load applications and residential loads are non-linear loads (Subjak et al., 1998; Khalid and Dwivedi, 2011; Sangepu and Vijay Muni, 2015). The consumer loads that are generally used in everyday life, both expensive and heavy loaded, are air conditioners, geysers, washing machines, and refrigerators. These non-linear loads are more prone to disturbances like harmonics, voltage sag and voltage swell are less resilient to these PQ problems (Elphick et al., 2017; Emanuel et al., 1999; Kumar and Zare, 2014). The definition of PQ is “any power problem manifested in voltage, current or frequency deviations that result in failure

or miss-operation of customer equipment” (Dao et al., 2015; Gao et al., 2017; Wagh and Singh, 2019; Baggini, 2008). Hence, this work focuses on providing a methodical practice to provide a solution such as an active power filter for the issue of harmonics that is present in the system, capable of placing our expensive appliances at risk. The model can be used to reference any common man with an intermediate level of understanding of electrical and electronics (Mikkil and Panda, 2015; Dugan et al., 2004; Niitsoo et al., 2010; Malik et al., 2021).

The productivity and profit of the major industries mainly depend upon modern semiconductor technology. All the systems based on semiconductor devices are designated to offer clean power. Even though, most of the controllable switches in the system increase the smartness of the system, non-linearity in the system may result in the disturbances of power such as the presence of harmonics and also increase the demand for reactive power (Sahoo, 2021; Jerin and Siano, 2018; Yahya et al., 2020). A pure sinusoidal supply voltage is necessary for systems with such types of sensitive loads. The system has to be maintained clean power in order to obtain the maximum efficiency and also to achieve the PQ issues as per the standards derived by the international standards (DaviCuriBusarello et al., 2016; Michaels, 1997; Anon., 1993).

* Correspondence to: Technological University Dublin, Park House, 191 N Circular Rd, Cabra East, Grangegorman, Dublin, D07 EWW4, Ireland.

E-mail addresses: thamizht@srmist.edu.in (T.M.T. Thentral), palanisr@srmist.edu.in (R. Palanisamy), ushakarthick@gmail.com (S. Usha), mohitbajaj@nitdelhi.ac.in (M. Bajaj), hossam.elsayed@tudublin.ie, hossam.zawbaa@gmail.com (H.M. Zawbaa), skamel@aswu.edu.eg (S. Kamel).

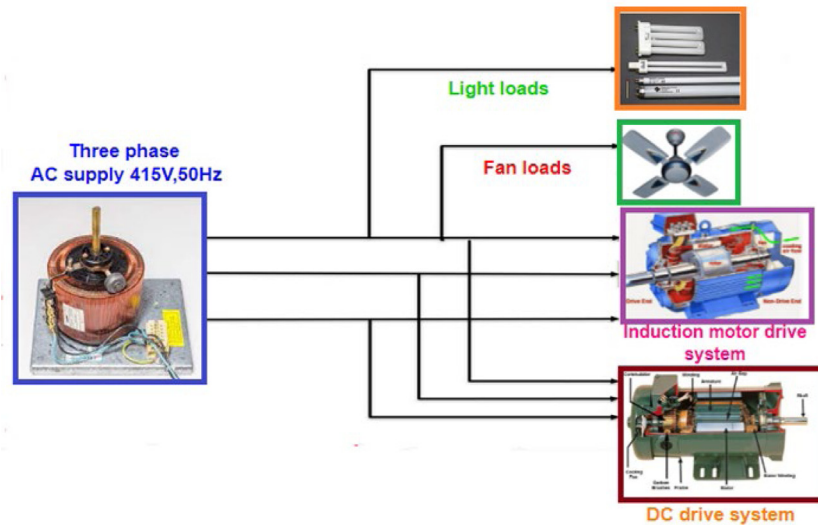


Fig. 1. Different load systems.

In most industrial, commercial and domestic applications, power electronic devices place a vital role. The non-linearity of these power electronic switches causes PQ issues (Swamy, 2015; Cho and Cha, 2011). Power electronic devices have now seamlessly integrated into every aspect of our life, including residential applications such as televisions, personal computers, etc.; Industrial apparatus such as Adjustable Speed Drives (ASDs), Programmable Logic Controllers (PLCs), Computerized Numerical Control (CNC) tools, rectifiers, inverters, etc. Business workplace equipment such as printers, copiers etc., PQ problems might be identified by the use of certain symptoms denoted below (Zobaa et al., 2010; Diwan et al., 2010; Kumar and Mishra, 2014).

The three major aspects of Power Electronics (PE) in power distribution are

- Many industrial and domestic equipment are designed with PE
- Notches, neutral currents, harmonics and inter-harmonics are caused by PE
- Many power quality problems are mitigated by PE.

Power electronic converters related equipment like switched-mode power supplies, varying frequency devices, computers, battery chargers and electronic ballasts create dominant harmonics (Hamadi et al., 2010; Al-Zamil and Torrey, 2000). In due course, it causes a lot of monetary losses. Due to this, there has been a great concern among power suppliers and consumers towards compensation techniques and PQ problems. The inception of harmonics is a buzz word from the late 20th century, which has continuously threatened the power system's regular working. The harmonics will distort voltage and current waveforms, which in turn creates overheating and nuisance tripping of the equipment. These are the reasons for the increasing interest in PQ (Wang et al., 2020; Chen et al., 2016; Su et al., 2018) issues.

The harmonics modeling for residential load considered experimental setup was developed in the National Instruments data acquisition (NI DAQ) module and a virtual instrument developed in LabView. The parameters such as active power and displacement power factor are obtained with the help of a power quality analyzer to achieve the true power factor (Karanki and Geddada, 2013; Zhong and Hornik, 2013; Farooq et al., 2011). There were 120 possible combinations of electrical loads are considered. In this, 120 combinations of loads minimum three combinations of loads are in the working conditions all the times in the micro-grid. The values obtained from the load patterns affect the quality

of the power (Blazek et al., 2020). The effect on power quality due to various residential appliances is discussed. The technology enhancement in home appliances majorly affects the quality of the power. The various electrical parameters such as voltage, current, frequency and power are measured and analyzed using NI instruments with labview software (Kavitha and Subramanian, 4967; Arsov et al., 2012; Toader et al., 2014).

A test is conducted in a real-time system to monitor the various PQ issues. The experimental setup is arranged in our college laboratory by considering tubelights, fans, a DC Drive system and an AC Drive system. The loads were taken under different variations and were recorded simultaneously using the Fluke 434 Series II Energy Analyzer that helps even in storing real-time data. This data was transferred to the computer and the required values pertaining to the issue were filtered out. The results obtained from the different load conditions are investigated and the SRF control technique rectifies the identified problems in the proposed work.

2. Analysis of power quality issues in real-time setup for different load conditions

The proposed work focuses on the analysis of PQ issues in the residential load systems and the Amada-AE2510NT turret punch CNC machine incorporated with multiple single-phase AC servo motor drive systems. In case one, laboratory setup is considered with different fan, light, AC and DC drive systems. In case two, the test is conducted on a real-time punch machine meant for different processes.

2.1. Residential load systems

An AC drive system, DC drive system, light loads and fan loads are considered for this work. A laboratory setup is implemented with these loads to monitor the various parameters like source voltage, source current, fundamental supply frequency, and power factor on the source side, also active power and reactive power. The light and fan loads are connected in 'R' phase along with the three-phase AC and DC drive system to create unbalance in the supply side. Fig. 1 shows the block diagram representation of different loads. A three-phase AC supply is applied by using three-phase autotransformers.

There are 8 cases that were taken under different loaded conditions for focusing on specific PQ issue that plays a key role

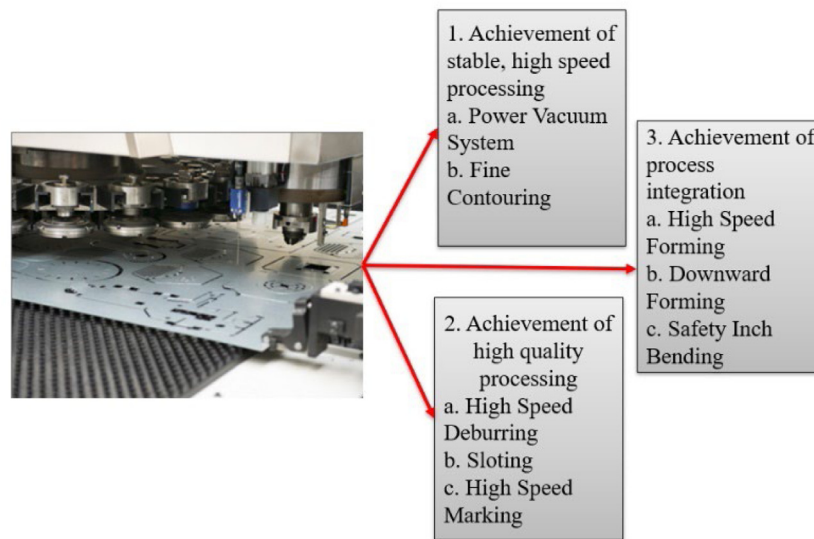


Fig. 2. Various functions of CNC machine.

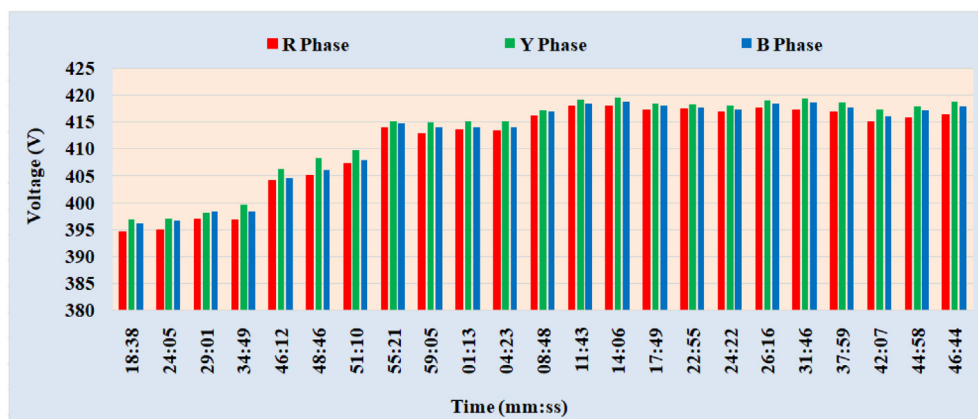


Fig. 3. Three-phases source voltage in residential loads.

in industries such as harmonics, transients, long and short duration voltage variations, voltage imbalance, etc. By testing done with the different load with loaded and unloaded conditions, the harmonic issue has been taken on the supply side with loads such as lights, fans, DC drive and AC drive.

With the use of a fluke analyzer, the % THD for different harmonic orders was taken for the above 8 cases. Table 1 shows the different loads and their ratings. The test has been undergone in a different time period with various loads, as shown in Table 2. The various parameters such as source voltage, source current, power factor, supply frequency and the total harmonic distortion of source voltage and current are monitored with the help of a fluke analyzer.

As mentioned in Table 1, the loads are connected to the supply one by one. Then, the combination of different loads is operated in a different time period to monitor the variations in different parameters. The AC and DC drives considered for testing are operated in loaded and unloaded conditions.

After conducting the experiment in the laboratory setup, the experiment is carried out in the real-time system to notice the variations in the voltage, current and other parameters. The Amada-AE2510NT turret punch CNC machine incorporated with multiple single-phase AC servo motor drive system in industry for different applications such as forming, deburring, downward marking, slotting, safety inch bending and fine contouring is

taken to monitor the variations and unbalance in the three-phase supply system of various parameters such as voltage, current, frequency, power factor and total harmonic distortion of voltage and current on the source side. One metal sheet with different thicknesses required for the application is subjected to the achievement of stable, high speed, high quality and integration processing. The minimum time period required to complete one sheet for the various process is designed as 30 min. Each process in the CNC machine is implemented with individual single-phase AC servo motors. Every motor in the machine is operated at different speeds for a particular time period. The various process of CNC machine is shown in Fig. 2 to explain the operating conditions of each single-phase AC servo motor incorporated in the machine.

3. Analysis of power quality issues in different load conditions

The different loads are switched on in different time periods and the variations in voltage, current, frequency, power factor and total harmonic distortion in current and voltage are recorded using a power quality analyzer. The source-side voltage for different load combinations is shown in Fig. 3. According to Fig. 3, it is more accurate to state that the three-phase source voltage is unbalanced regardless of non-linear loads connected to the power system. The load is switched on with different time periods.

Table 1
Different load combinations and rating.

S. No	Load details	Load condition	Quantity
1	Fluorescent light	Unloaded	14
2	Ceiling fan		7
3	Fluorescent light + Ceiling fan		14 Fluorescent lights 7 Ceiling fans
4	AC motor drive		1 AC motor - 3 phase squirrel cage induction motor
	Speed 1 = 1005 RPM		Make: SIEMENS, Insl: 'F' Class
	Speed 2 = 1200 RPM		Frequency: 50 Hz Speed: 1435 RPM
	Loaded - 1200 rpm		Amps: 4.4 A ; Volts: 415 V (delta)
	Load 1 = 2 kg		Power: 2.2 kw, 3 HP
5	DC motor drive	Unloaded	Make: 1 DC motor - DC Shunt Motor
	Speed 1 = 500 RPM	Speed 1 = 500 RPM	BEN EleInsl: 'B' Class
	Loaded - 450–420 rpm	Loaded - 450–420 rpm	Frequency: 50 Hz
		Load 1 - 3 kg	Speed: 1500 RPM
		Load 2 = 4 kg	Amps: 19 A DC Volts: 220 V
6	Fluorescent light + Ceiling fan + AC motor drive	Unloaded	Power: 3.7 kw, 5 HP
			14 Fluorescent lights
			7 Ceiling fans
			1 AC motor
		Speed 1–1005 RPM	
		Speed 2 - 1200	
		Loaded	
		Load 1 - 2 kg	
		Load 2 - 3 kg	
7	Fluorescent light + Ceiling fan + AC motor drive + DC motor drive	Loaded	14 Fluorescent lights
		Load 2 (3 kg) (AC = 1200 rpm) > Load 2 (2 kg) (DC = 1200 rpm)	7 Ceiling fans
		Load 2 (3 kg) (AC = 1200 rpm) = Load 2 (3 kg) (DC = 1200 rpm)	1AC motor
		Load 2 (3 kg) (AC = 1200 rpm) < Load 2 (4 kg) (DC = 1200 rpm)	1 DC motor
8	AC motor drive + DC motor drive	AC - 1000 rpm unload DC - 420 rpm 4 kg	14 Fluorescent lights
		UnLoaded	7 Ceiling fans
		Speed 1–1000; Speed 2 = 500 rpm	1 AC motor
		Loaded	1 DC motor
		Load 2 (3 kg) (AC = 1000 rpm) > Load 2 (2 kg) (DC = 480 rpm)	
		Load 2 (1 kg) (AC = 1000 rpm) = Load 2 (1 kg) (DC = 450 rpm)	
		Load 2 (1 kg) (AC = 1000 rpm) < Load 2 (2 kg)(DC = 420 rpm)	

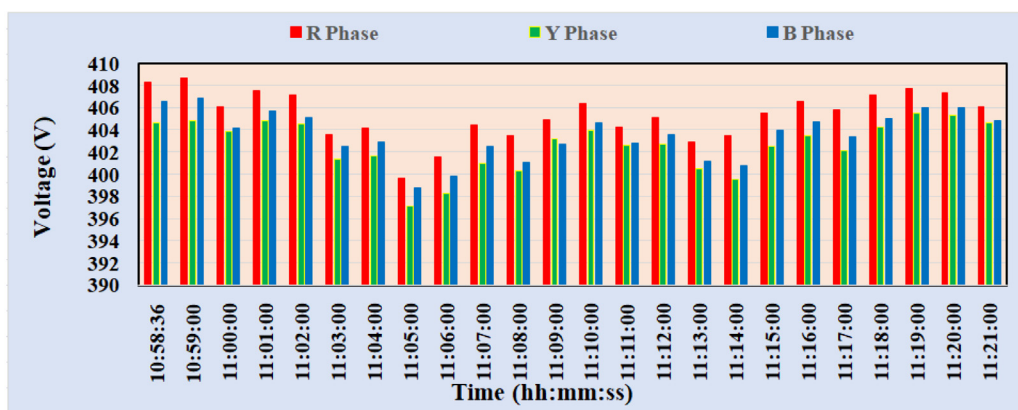


Fig. 4. Three-phase source voltage in servo motor systems.

Initially, the light load alone switched on. The voltage at that condition is a maximum 395 V for the three-phase supply voltage of 415 V. Likewise, the second load Fan is switched on 24 min and 04 s. Then light and fan loads are connected to the system. In the same manner, the experiment is continued for four types of individual loads as well as combinations of two loads, three loads and finally with all the four loads. According to the variations in the load on the distribution end, the voltage also varied. From

the observation of voltage in different load patterns, the source voltage has been varied from 395 V to 420 V. The diagram depicts that the voltage in all three-phases is not the same.

Fig. 4 shows the source voltage profiles of real-time servo motor systems performing different processes. Depending upon the functioning of the real-time system, the source voltage is varied. When the process of the machine changes based on the single-phase AC servo motor for the particular process, the voltage also

Table 2
Different load combinations vs time.

S.No	Load	Time	S.No	Load	Time
1	None	12:18:38	13	AC Drive (US1 - 1200)	13:11:43
2	Fluorescent light	12:24:05	14	AC Drive (LS1 - 1200, 2 kgs)	13:14:06
3	Ceiling fan	12:29:01	15	AC Drive (LS2 - 1200, 3 kgs)	13:17:49
4	Fluorescent light + Ceiling fan	12:34:49	16	DC Drive (US1 - 500)	13:22:55
5	Fluorescent light + Ceiling fan + AC Drive (US1 - 1000)	12:46:12	17	DC Drive (LS1 - 450, 3 kgs)	13:24:22
6	Fluorescent light + Ceiling fan + AC Drive (US2 - 1200)	12:48:46	18	DC Drive (LS2 - 420, 4 kgs)	13:26:16
7	Fluorescent light + Fan + AC Drive (LS1 - 1200, 2 kg)	12:51:10	19	AC Drive + DC Drive (LS1 - Load 1 (0 kg) (AC = 1000 rpm); Load 2 (4 kg) (DC = 420 rpm))	13:31:46
8	Fluorescent light + Ceiling fan + AC Drive (LS2 - 1200, 3 kg)	12:55:21	20	AC Drive + DC Drive (US1 - Load 1 (0 kg) (AC = 1000 rpm); Load 2 (0 kg) (DC = 500 rpm))	13:37:59
9	Fluorescent light + Ceiling fan + AC Drive + DC Drive (LS2 - Load 1 (3 kg) (AC = 1200 rpm) = Load 2 (3 kg) (DC = 1200 rpm))	12:59:05	21	AC Drive + DC Drive (LS2 - Load 1 (3 kg) (AC = 1000 rpm) > Load 2 (2 kg) (DC = 420 rpm))	13:42:07
10	Fluorescent light + Ceiling fan + AC Drive + DC Drive (LS3 - Load 1 (3 kg) (AC = 1200 rpm) < Load 2 (4 kg) (DC = 1200 rpm))	13:01:13	22	AC Drive + DC Drive (LS3 - Load 1 (1 kg) (AC = 1000 rpm) = Load 2 (1 kg) (DC = 450 rpm))	13:44:58
11	Fluorescent light + Ceiling fan + AC Drive + DC Drive (LS1 - Load 1 (3 kg) (AC = 1200 rpm) > Load 2 (2 kg) (DC = 1200 rpm))	13:04:23	23	AC Drive + DC Drive (LS2 - Load 1 (1 kg) (AC = 1000 rpm) < Load 2 (2 kg) (DC = 420 rpm))	13:46:44
12	AC Drive (US1 - 1000)	13:08:48			

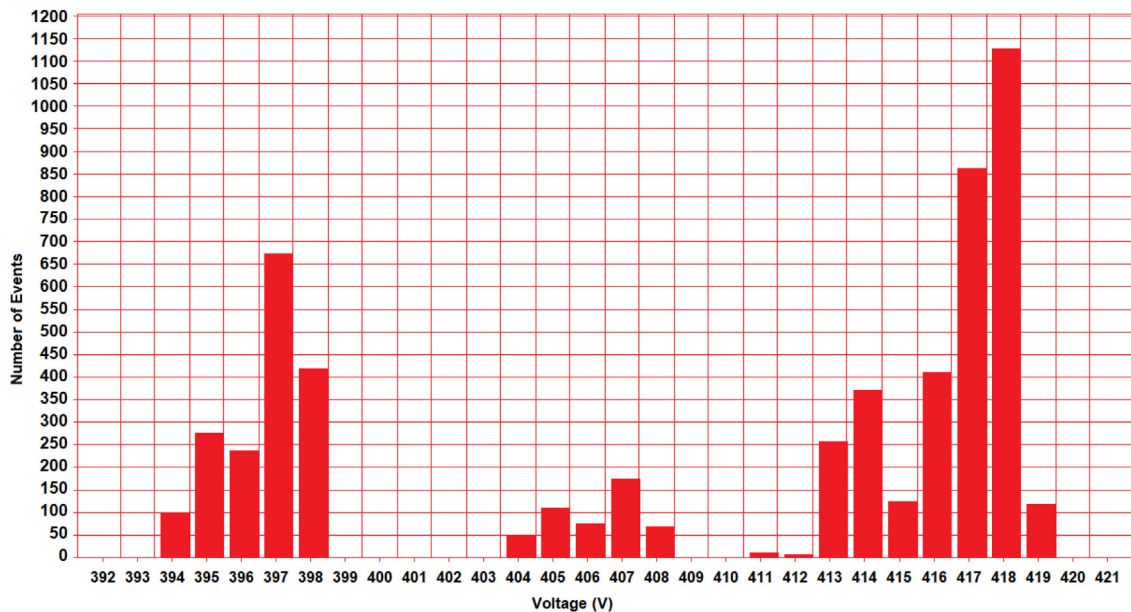


Fig. 5. Variations in source voltage per phase with residential loads.

varies at the source side. Each time period in the graph represents each process in the CNC machine. It also shows that the voltage is not the same in all three-phases. The peak value of the voltage varies from 398 V to 408 V.

When the system load is subjected to change, the three-phase source voltage also varies accordingly. The bar graph in Fig. 5 depicts the variations that occurred in the residential load. The system is monitored through a fluke analyzer for each millisecond 1100 events are recorded. Based on the variations in the load, the peak value of the grid voltage is varied from 394 V to 419 V. The upper extreme value of 419 V voltage has occurred in 110 events. Likewise, the lower extreme value of 394 V occurs in

more than 100 events. In the same manner, the upper and lower extreme values of the real-time system are shown in Fig. 6. The maximum and minimum values of the source voltage are 398.5 V and 409.5 V.

The variations and unbalance in the three-phase source current for different load conditions and real-time servo motor systems are shown in Figs. 7 and 8. It is observed that in a laboratory setup, the unbalance in current is more for the light and fan load with AC and DC drive system. The unbalance three-phase current condition is more severe than the unbalance three-phase voltage condition when the system was connected to the residential non-linear loads. The maximum current recorded for that load is 8 A.

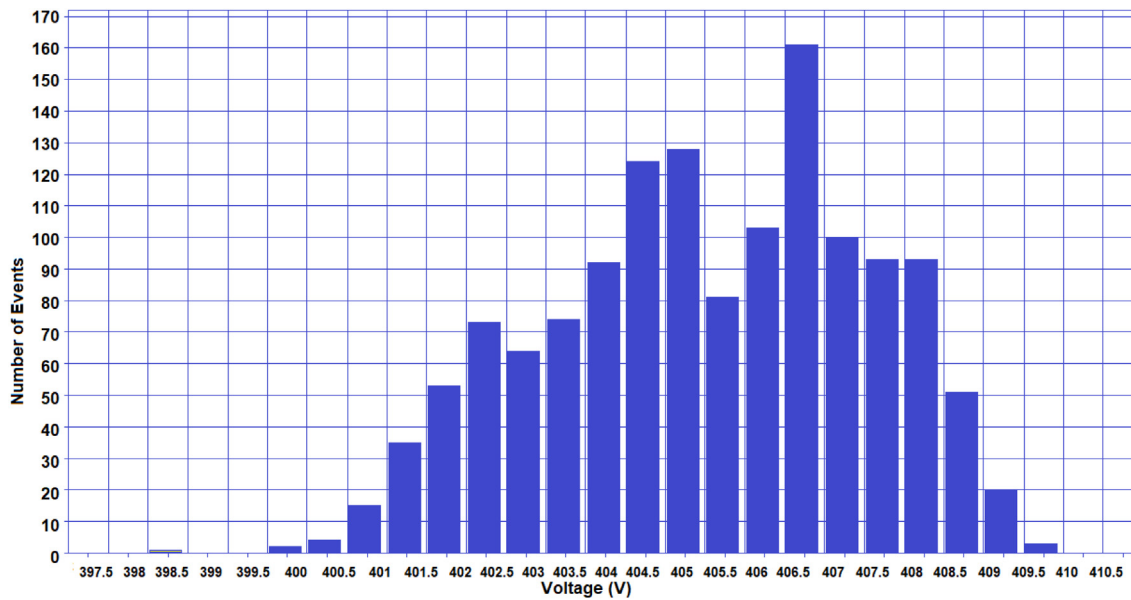


Fig. 6. Variations in source voltage per phase for servo motor systems.

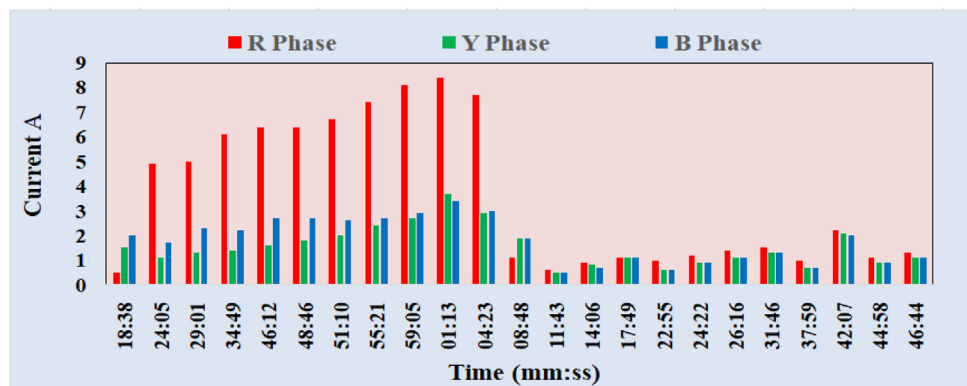


Fig. 7. Unbalance and variations in 3-phase source current for residential loads.

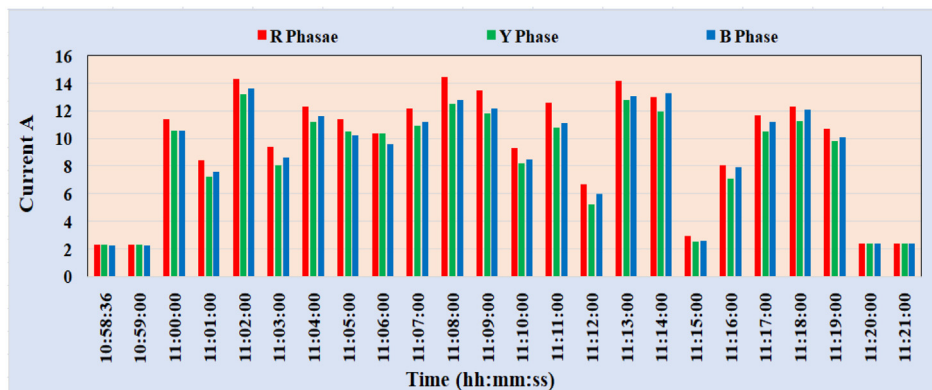


Fig. 8. Unbalance and variations in source current for servo motor systems.

Only for the load of the drive, the variations and unbalance in current is very less. The variations and unbalance in the three-phase source current for different load conditions are shown in Fig. 8. It shows that due to the various functioning of CNC machines, there

are more variations and unbalances in the current. The maximum current recorded for that load is 13 A.

The bar graph in Fig. 9 shows the current's upper and lower extreme values of current based on the change in loads. The upper

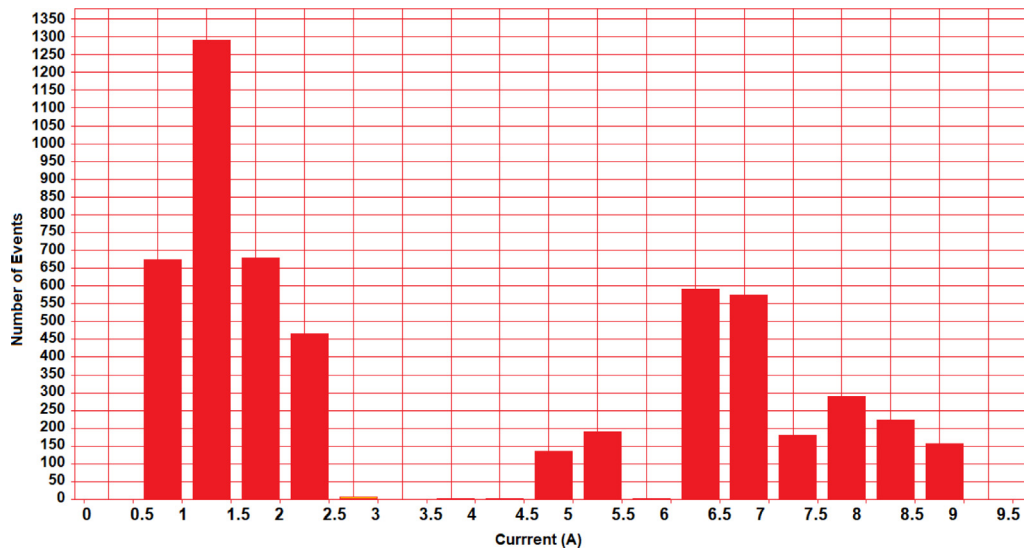


Fig. 9. Variations in source current per phase with for residential loads.

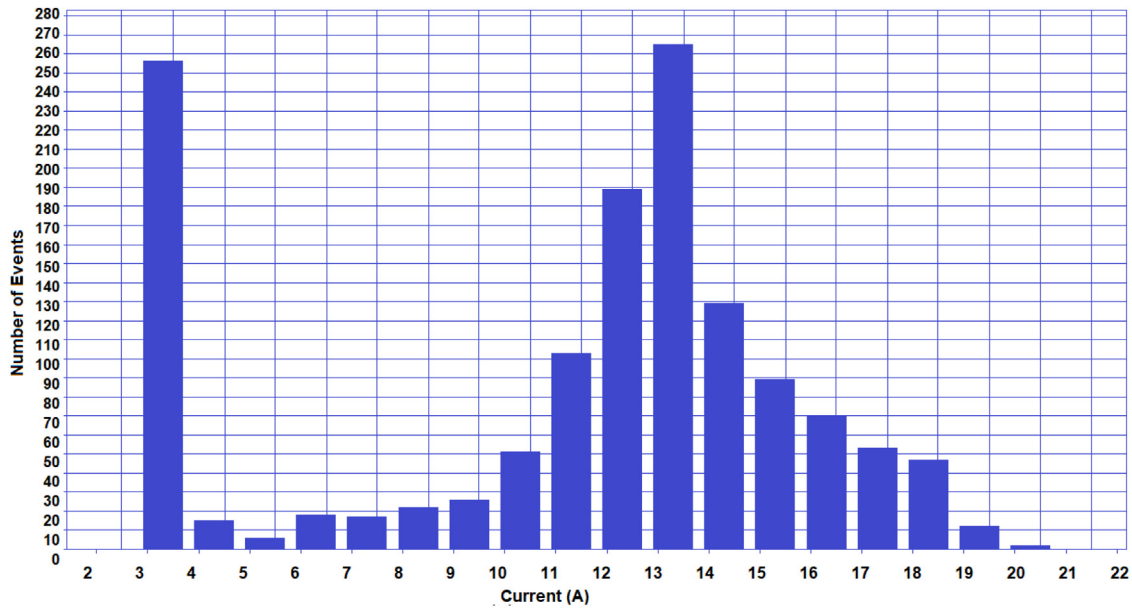


Fig. 10. Variations in source current per phase for servo motor systems.

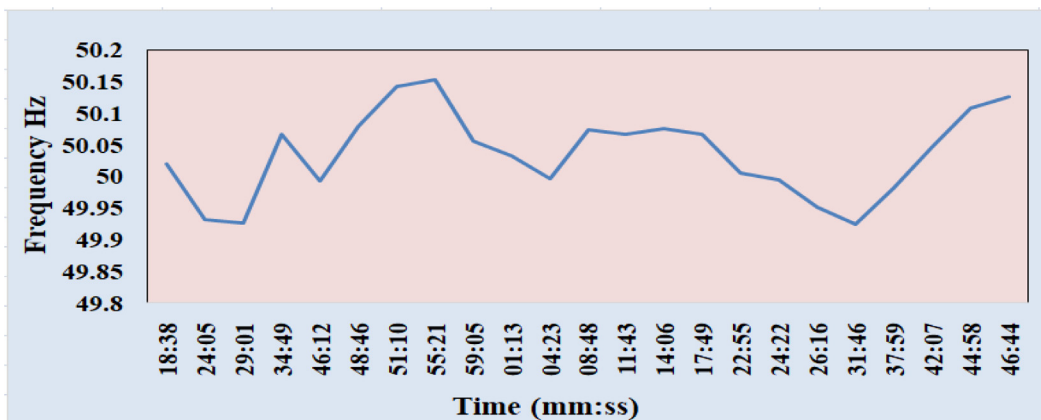


Fig. 11. Oscillations in supply frequency vs time with residential loads.

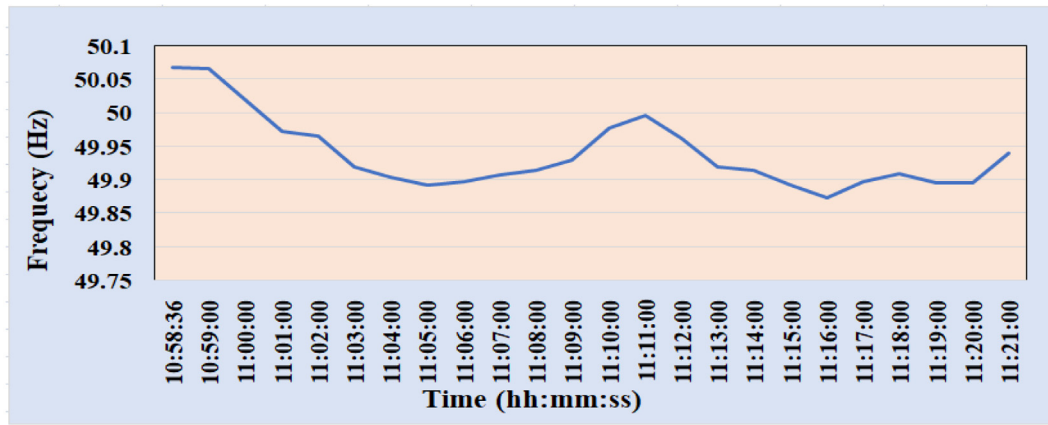


Fig. 12. Oscillations in source frequency vs time for servo motor systems.

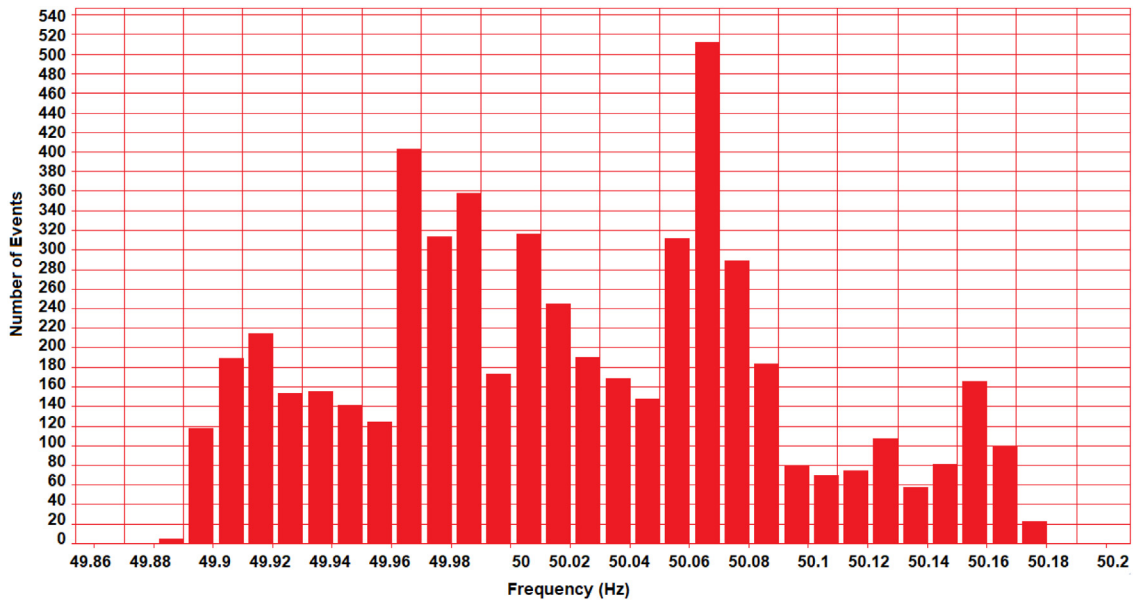


Fig. 13. Variations in frequency with residential loads.

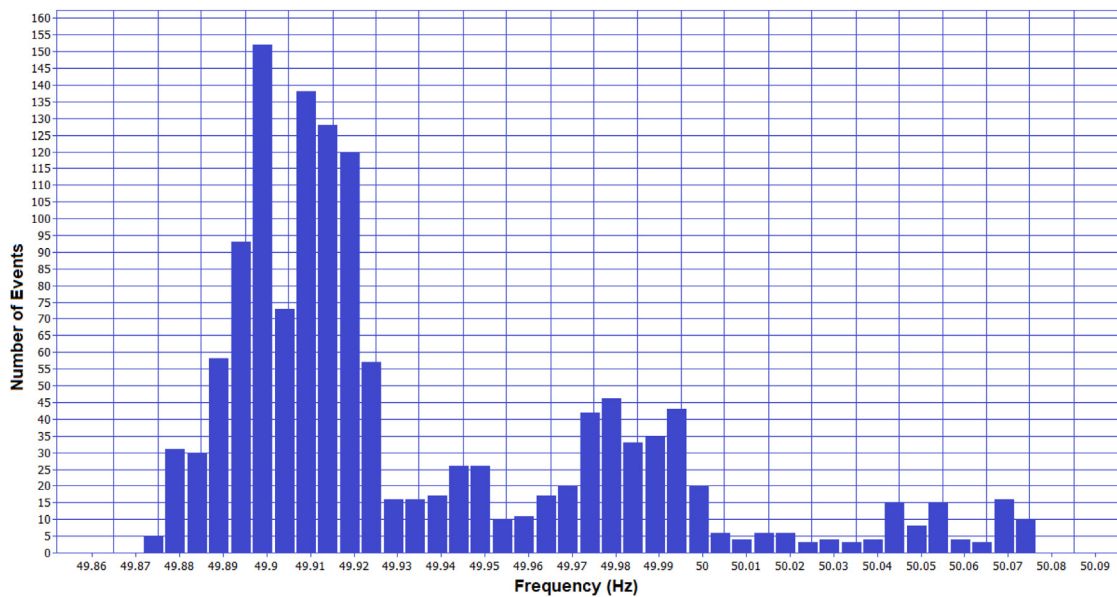


Fig. 14. Variations in frequency with for servo motor systems.

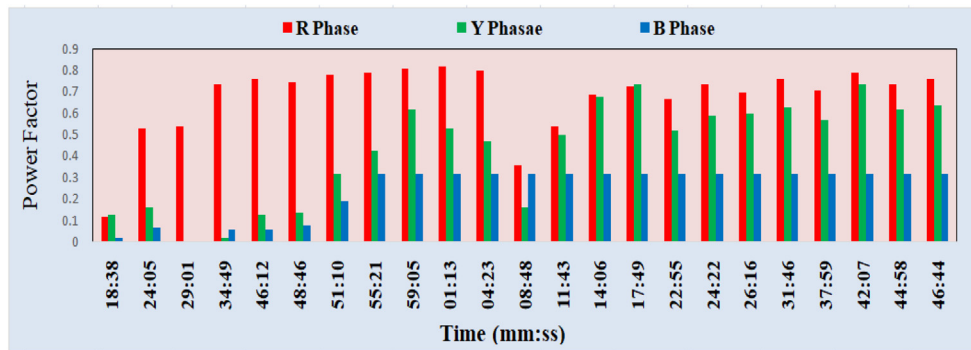


Fig. 15. Unbalance and variations in power factor for varying load case.

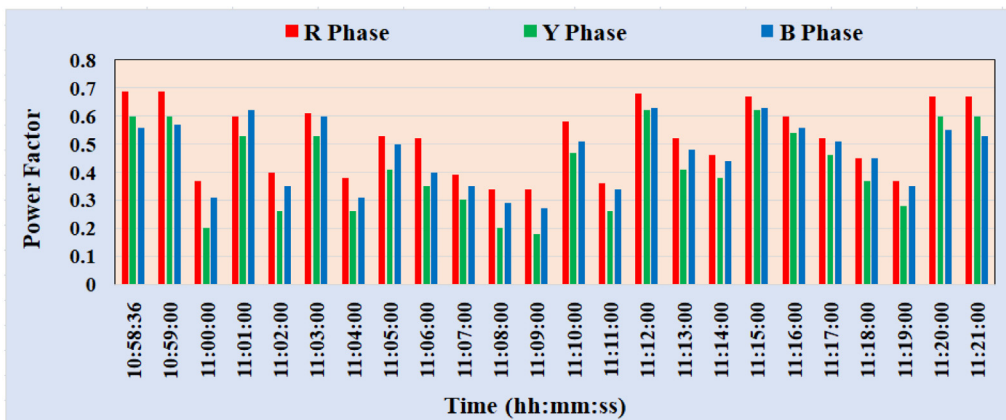


Fig. 16. Unbalance and variations in power factor for servo motor systems.

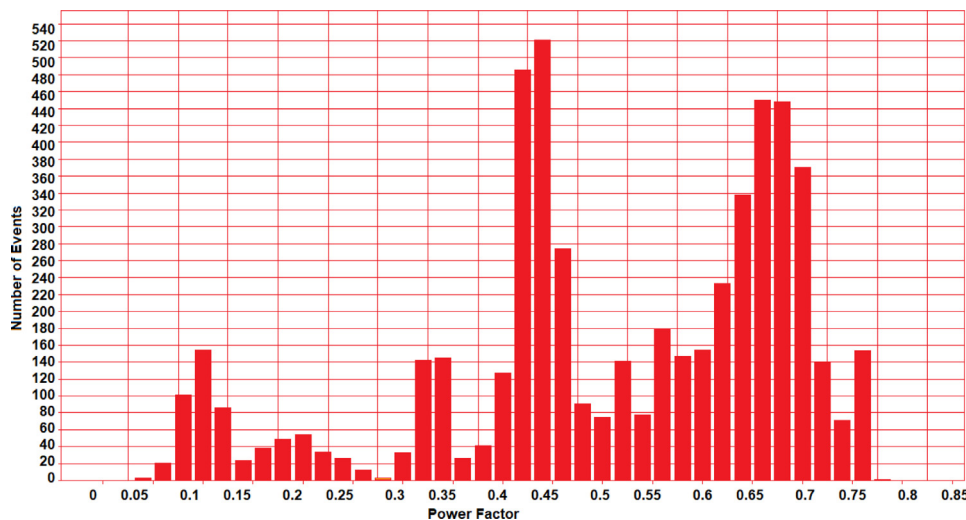


Fig. 17. Variations in power factor with residential loads.

extreme value is 8.4 A and the lower extreme value of source current is 0.3 A. The number of events that appeared is 1350.

The bar graph in Fig. 10 shows the current's upper and lower extreme values. The upper extreme value is 20.2 A and the lower extreme value of source current is 2.3 A. The number of events that appeared is 1350. The 95 percentile of source current in a maximum event is 17.1 A.

Due to the different functions of the machine, there is a speed variation in the drive system. Due to which the variations are present in the frequency in different load conditions and real-time systems, the same is shown in Figs. 11 and 12.

The fundamental frequency is varied from 49.925 Hz to 50.152 Hz. Figs. 13 and 14 show the bar graph of frequency variations in different load conditions and real-time systems. Due to load variations in both systems, frequency is varied. However, it is within the IEEE standards.

Figs. 15 and 16 depict the unbalance and variations in the power factor in different loaded conditions. The minimum power factor is 0.05 and the maximum power factor recorded in the power quality analyzer is 0.95. The number of events that appeared in this system is 1350. In this power factor 0.75 has appeared in a maximum number of events. In the laboratory

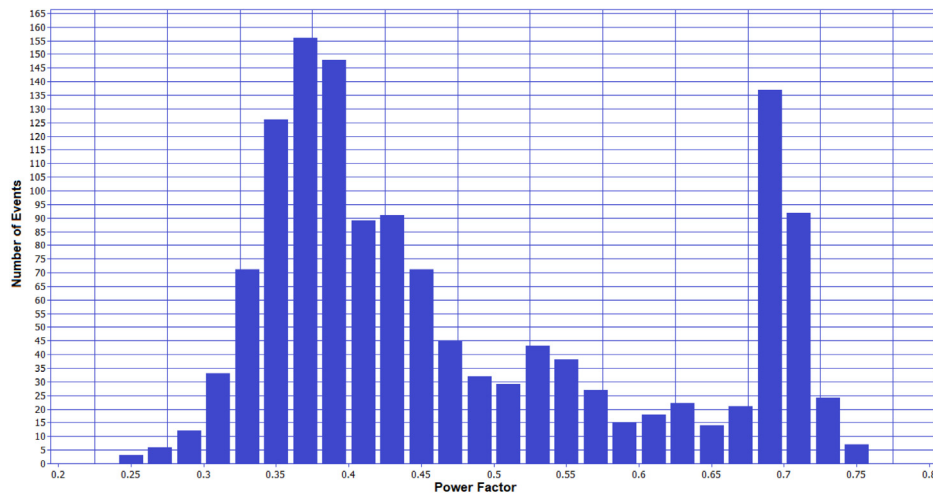


Fig. 18. Variations in power factor for servo motor systems.

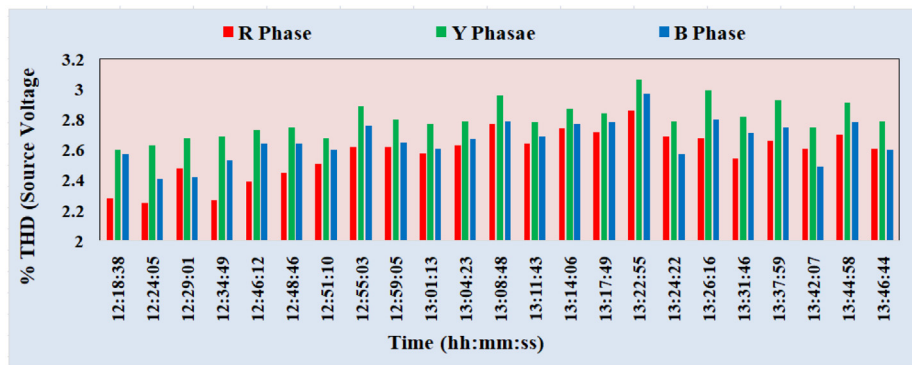


Fig. 19. % THD of source voltage with residential loads.

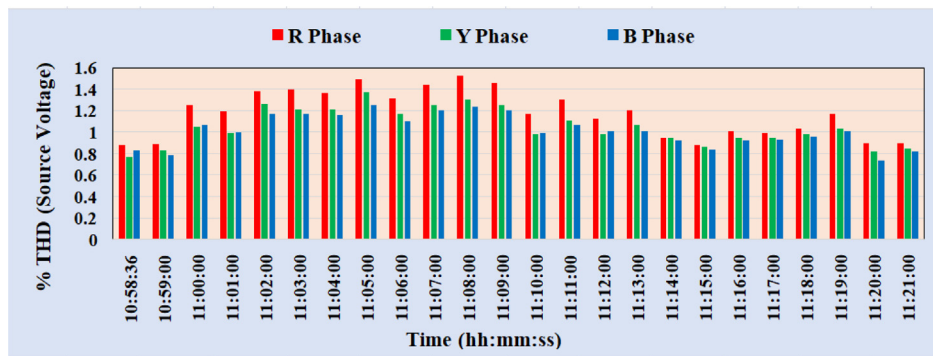


Fig. 20. % THD of source voltage for servo motor systems.

experiment due to the unbalance in the distribution of loads in the three-phase causes a large unbalance in the phases.

Figs. 17 and 18 give the unbalance and variations in the power factor in a real-time system. The minimum power factor is 0.25 and the maximum power factor recorded in the power quality analyzer is 0.75. In a real-time system, the power factor reduced much compared to the laboratory experiment conducted for different loaded conditions.

The variations and unbalance in % THD of Source voltage in both different loaded conditions and real-time systems are shown in Figs. 19 and 20. For the different loaded conditions, the bar graph in Fig. 19 depicts that the maximum % THD of the source voltage is up to 3%. For the real-time system, the bar graph in

Fig. 20 depicts that the maximum % THD of the source voltage is up to 1.5%. The % THD of source voltage in both systems is within the IEEE standard recommended value. It clearly explains that the % THD of the source voltage is not increased for the variations in load.

The variations and unbalance in % THD of Source Current in both different loaded conditions and real-time systems are shown in Figs. 21 and 22. For the different loaded conditions, the bar graph in Fig. 22 depicts that the maximum % THD of source current is up to 120%. For the real-time system, the bar graph in Fig. 23 depicts that the maximum % THD of source current is up to 70%.

The variations in active power in both different loaded conditions and real-time systems are shown in Figs. 23 and 24. The bar

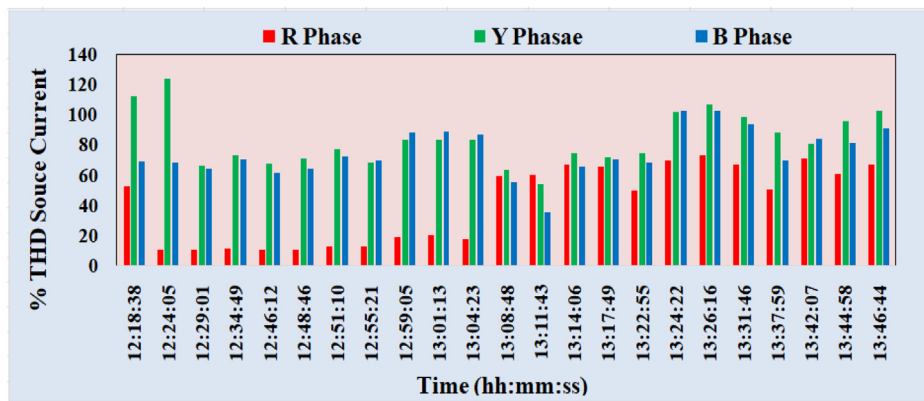


Fig. 21. % THD of source current with residential loads.

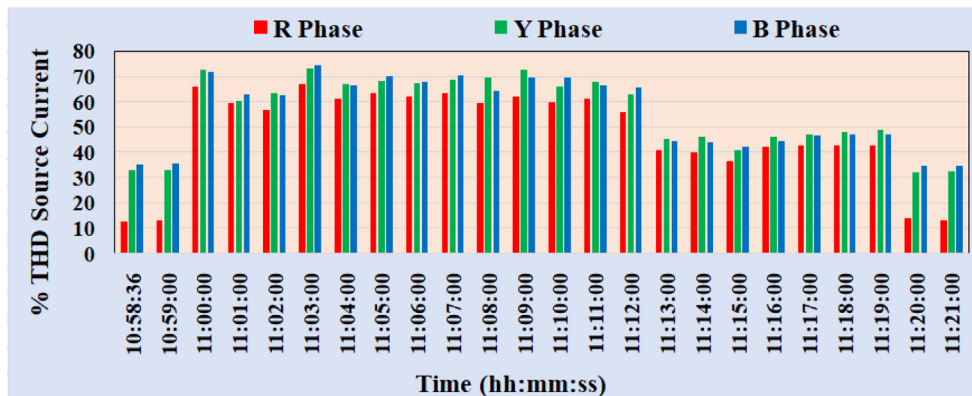


Fig. 22. % THD of source current for servo motor systems.

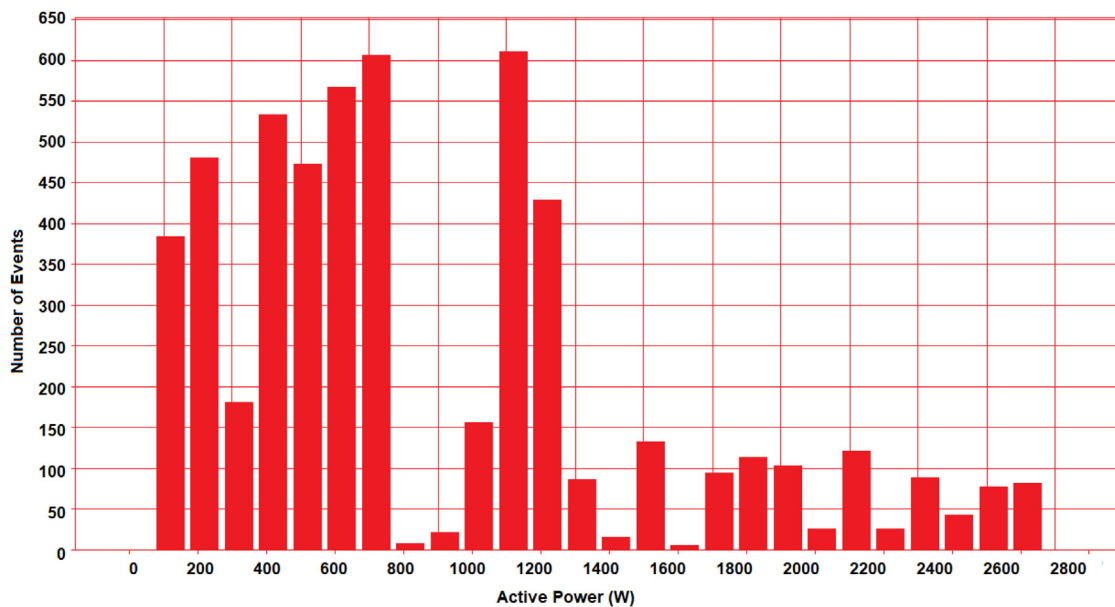


Fig. 23. Variations in active power with residential loads.

graph in Fig. 23 explains that the maximum active power value is 1660 W and the minimum value of active power is 10 W. The active power of 1530 W has appeared as 95 percentile. In a real-time system, the bar graph in Fig. 24 depicts that the maximum value of active power is 1820 W and the minimum value of active power is 280 W. The active power of 1320 VA has appeared as 95 percentile.

The variations in apparent power in both different loaded conditions and real-time systems are shown in Figs. 25 and 26. The bar graph in Fig. 25 depicts that the maximum value of apparent power is 2020 VA and the minimum value of apparent power is 60 VA. The apparent power of 1890 VA has appeared as 95 percentile. The bar graph in Fig. 26 depicts that the maximum value of apparent power is 4340 VA in a real-time system and

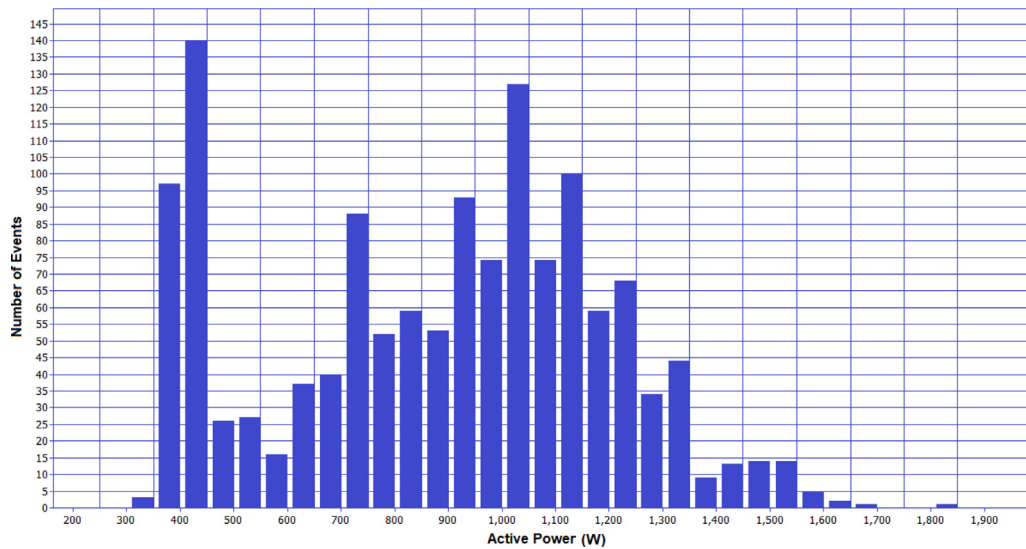


Fig. 24. Variations in active power for servo motor systems.

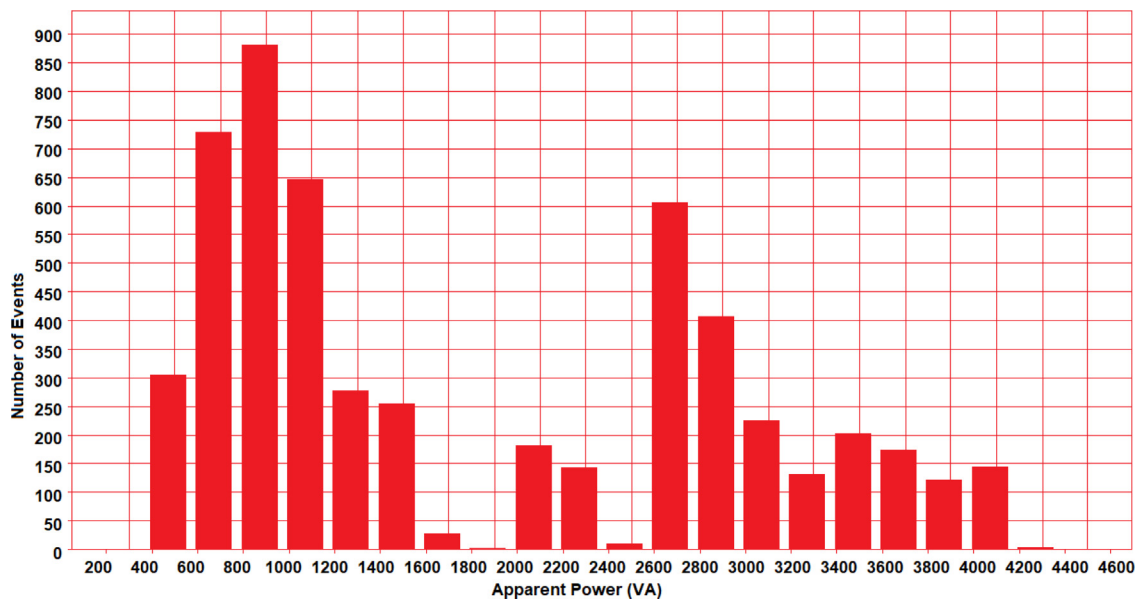


Fig. 25. Variations in apparent power with residential loads.

the minimum value of apparent power is 520 VA. The apparent power of 3760 VA has appeared as 95 percentile.

The Displacement Power Factor (DPF) variations in different load conditions are shown in Fig. 27. The number of events recorded in the analyzer is 1450. This lower extreme DPF monitored is 0.05, which appears in 350 events. Unity DPF has occurred in 1250 events. For the maximum number of events, the DPF is 0.8 that is appeared in 1400 events.

The variations in DPF in a real-time system are shown in Fig. 28. The upper extreme level of DPF is 0.88. It appeared in 5 events. The lower extreme level of DPF is 0.45. The maximum 95% of DPF is 0.66. The system is monitored through a fluke analyzer in every one millisecond.

The performance of laboratory setup on different load combinations such as light, fan and drive system and with a real-time system are analyzed. The Unbalance in supply Voltages Unbalance in supply Frequency, Reduction in Power Factor, Unbalance in the Source Current and current THD up to 70% has been analyzed. From the observations noticed from the analysis for different load

conditions, the following measures are to be taken. Mitigation of the current harmonics at the source side, compensation of reactive power, improvement in power factor, compensation of voltage increment or reduction occurred at the source side for a short duration of time and Regulation of unbalance in the voltage and current has been analyzed. The performance enhancement of PQ issues will be investigated with the implementation of an active filter in Matlab simulation and with experimental results to overcome the PQ issues identified from the real-time analysis.

4. Simulation results and discussion

The system is considered with AC induction motor drive load and uncontrolled rectifier load. The system is simulated in Matlab platform and the results obtained from the simulation are discussed. Shunt active power filter is used to mitigate the current harmonic that occurred due to the non-linear system. Fig. 29a shows the source voltage applied to the non-linear system. Three-phase three-wire system with harmonic producing load is simulated for one second. The source voltage is not affected by the

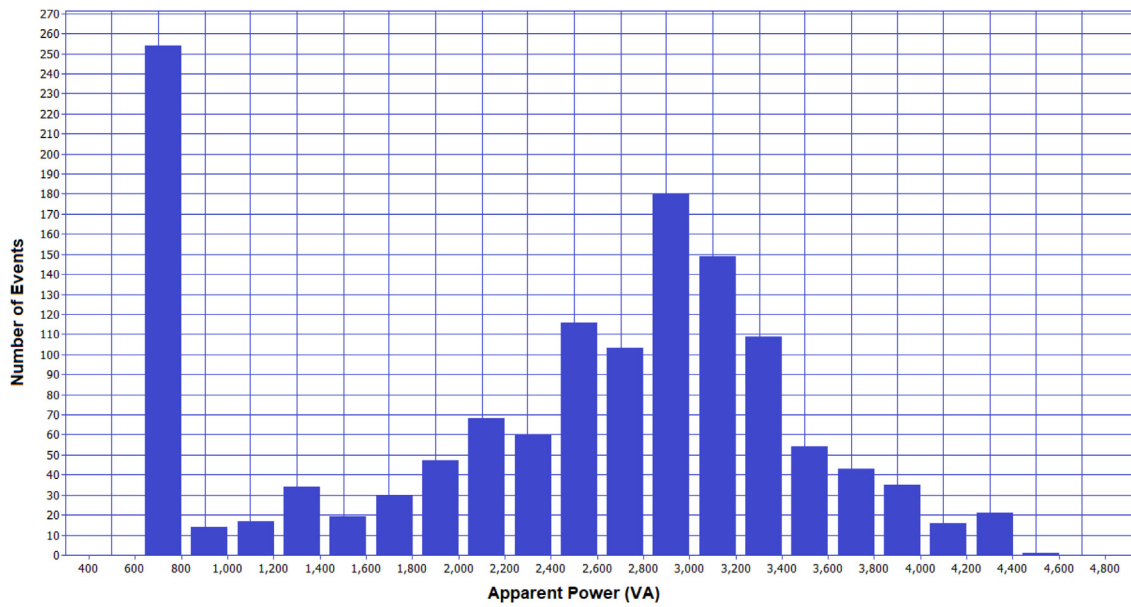


Fig. 26. Variations in apparent power for servo motor systems.

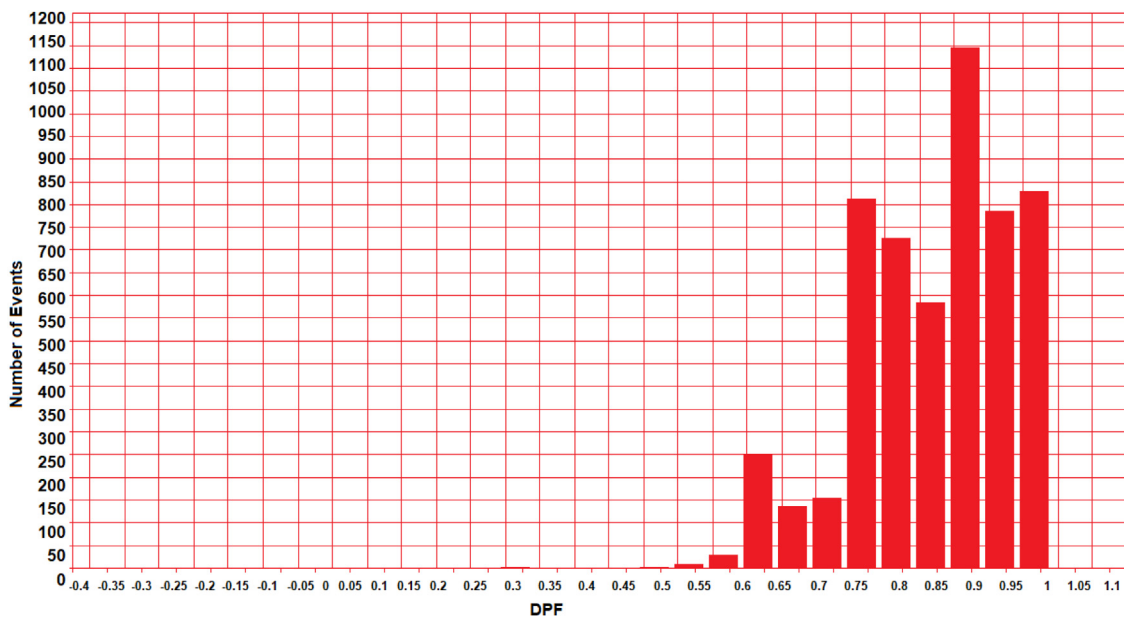


Fig. 27. Variations in displacement power factor with residential loads.

harmonic injecting load. Fig. 29b depicts the voltage at the load side. The filter is injected at 0.1 s.

Figs. 30a and 30b show the source current and filter current. When the filter is injected into the system, the source current becomes sinusoidal and also the harmonics present in the source current are eliminated, which is shown in Fig. 30a. The compensating current injected into the system is shown in Fig. 30b.

Fig. 31 represents the dc link capacitor voltage. At 0.1 s, the load connected to the system is an uncontrolled bridge rectifier. After 0.2 s, the system is loaded with both a rectifier and an AC drive system. The variations in filter current due to different load conditions are also depicted here. According to the variations in filter current, the DC link voltage also varied and obtained the constant value.

Both the loaded conditions, the source current % THD is within the IEEE 519 recommended standard value. The source is currently reduced to 1.07% after the filter is added to the system. Fig. 32 depicts the FFT analysis for source current with %THD of 1.07%.

4.1. Hardware implementation

The hardware implementation of three-phase supply system with induction motor drive load is shown in Fig. 33. Three-phase auto transformer is used to vary the supply voltage. 2 mH inductor is used at the source side to limit the current. The source current and voltage harmonics are noted by using the fluke analyzer. The waveform obtained from the three-phase systems is observed by the digital storage oscilloscope. The source

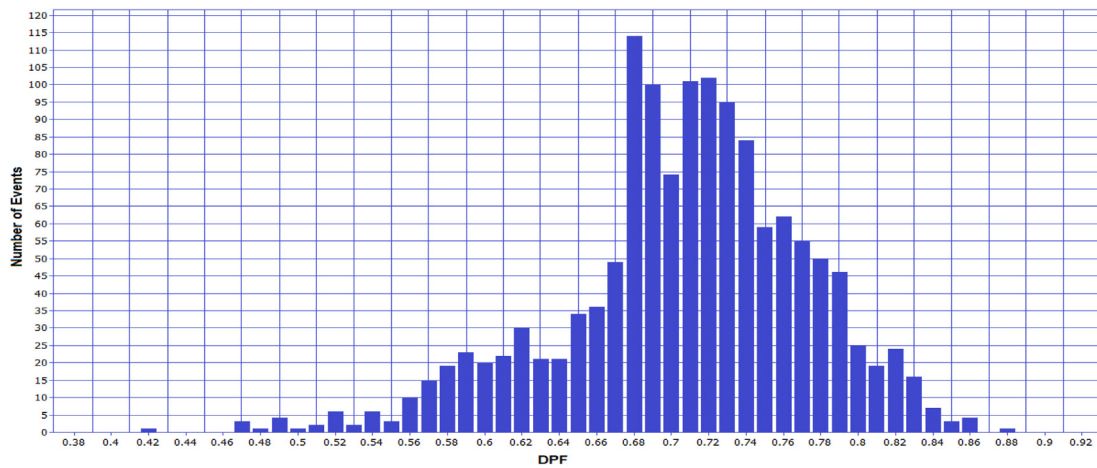


Fig. 28. Variations in displacement power factor for servo motor systems.

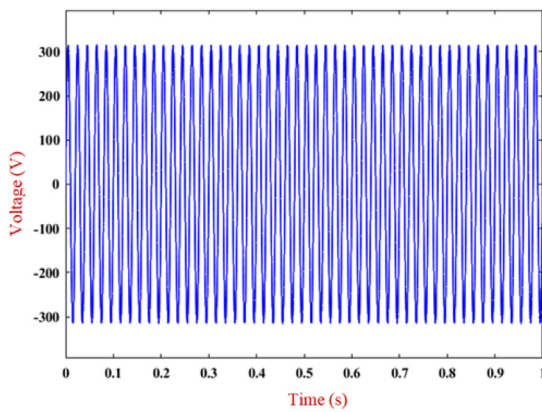


Fig. 29a. Source voltage.

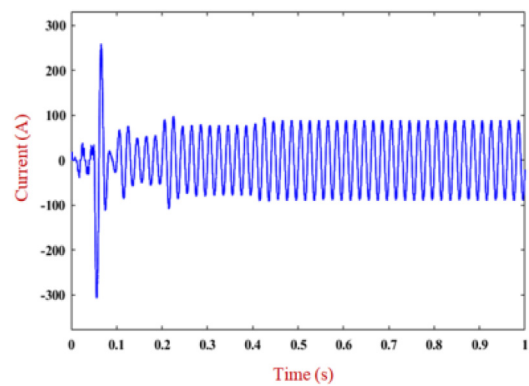


Fig. 30a. Source current.

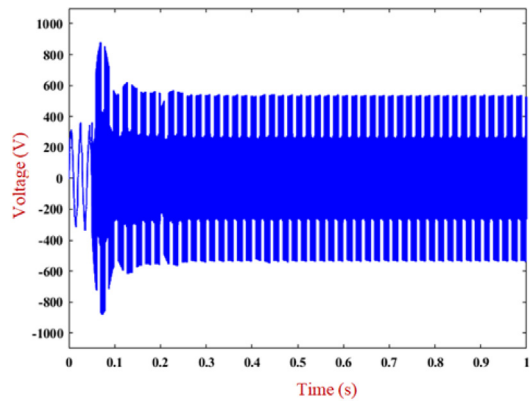


Fig. 29b. Load voltage.

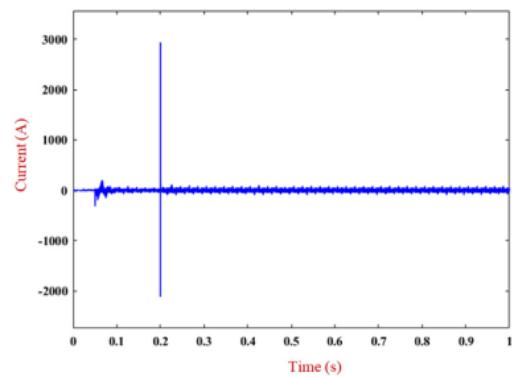


Fig. 30b. Filter current.

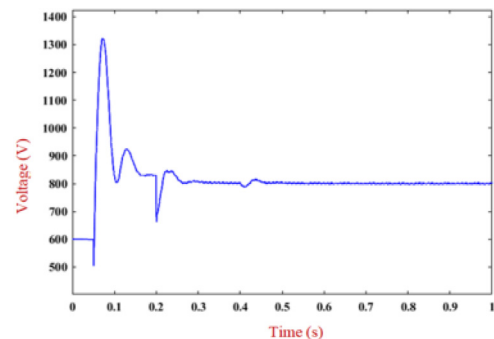


Fig. 31. DC link capacitor voltage.

voltage and current waveform, load side current and the filter for three-phase systems obtained from the hardware setup are shown in Fig. 34. It shows that before and after compensation, the source voltage is sinusoidal in shape. However, the source current before compensation is non-sinusoidal. Once the filter is injected, the source current becomes sinusoidal. At the same time, compensating current also increased in the filter current. Before that, the filter current is zero. In both cases, the load side current is non-sinusoidal only. The hardware output value obtained from the system is tabulated in Table 3.

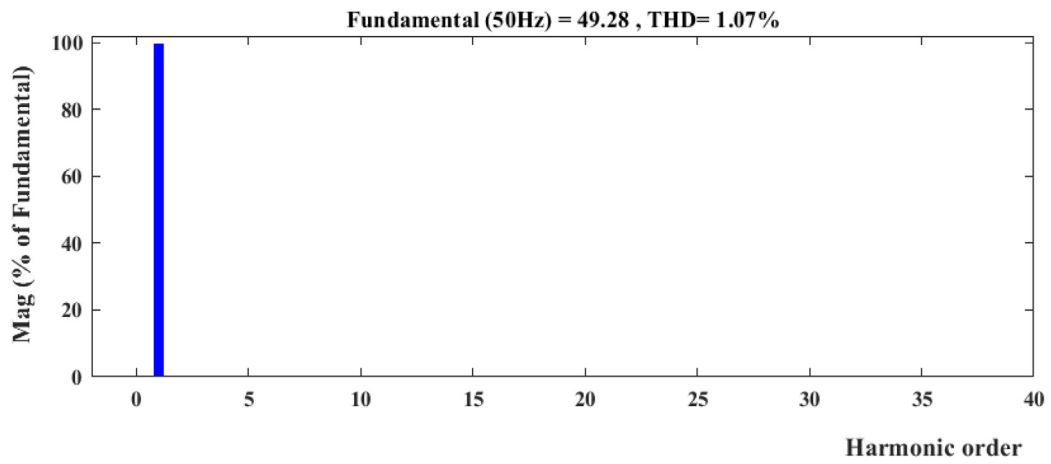


Fig. 32. % THD of source current.

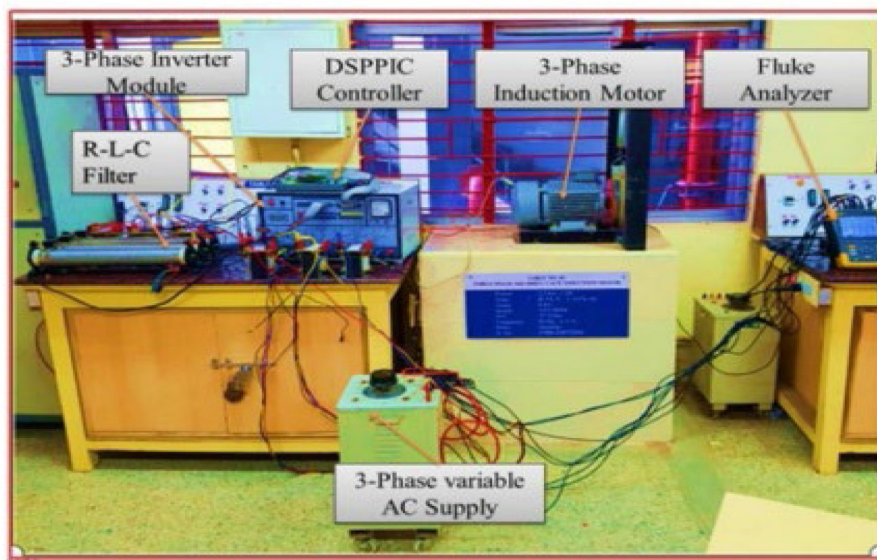


Fig. 33. Hardware implementation of induction motor drive load.

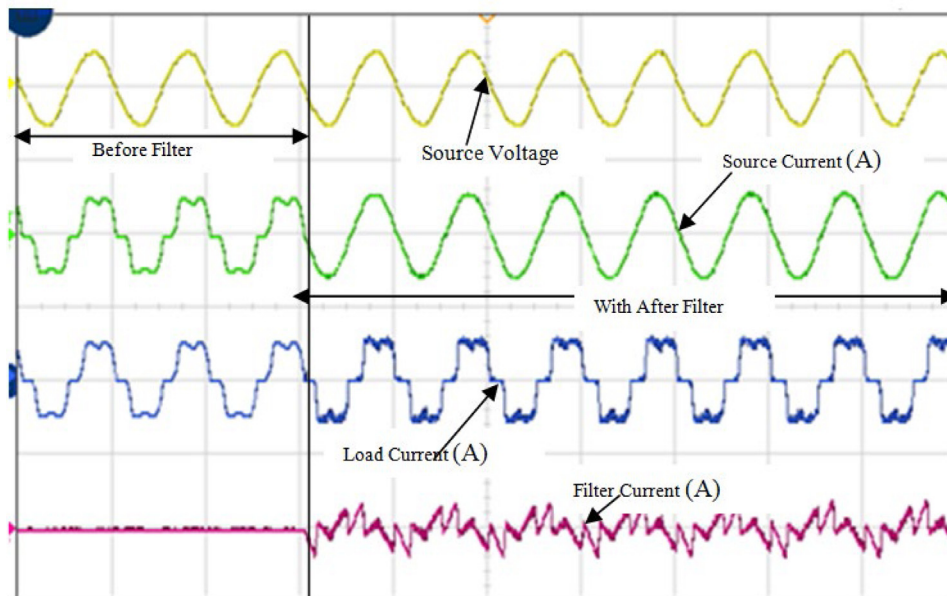


Fig. 34. Hardware outputs.

Table 3
Hardware output values.

Source voltage (V)	Source current (A)	Load side current (A)	Filter current (A)
70.9 RMS	4.15 RMS	4.2 RMS	1.5 RMS

5. Conclusion

To investigate the performance of various non-linear loads, the laboratory setup on different load combinations such as light, fan and drive system and real-time system is implemented. The variations occurred in the supply voltage, source current and frequency are monitored by using a fluke analyzer. Also, the variations in real power and apparent power are discussed in this paper. From the test conducted on the laboratory setup and real-time system, it observed that,

- ✓ The voltage on the source side is always unbalanced
- ✓ When the load is changing, the variations in the voltage and current occurred
- ✓ Due the drive system with the variable speed, the harmonics in the source current occurred and also the % THD also increases and it is not within the recommended standards.
- ✓ The load on the real-time system is intermittent load, so that the power factor is also reduced.

The reduction in power factor and current THD are monitored in both the lab setup and real-time load case study. The solution to the current harmonic at the source side, compensation of reactive power, improvement in power factor for two different load conditions are achieved by implementing the shunt active power filter. The simulation for the system with compensations is conducted and the %THD is reduced to 1.07%. Almost unity power factor is achieved. The same load condition is implemented in hardware and obtained the %THD as 2%.

CRedit authorship contribution statement

T.M. Thamizh Thentral: Data curation, Methodology, Software, Writing, Reviewing. **R. Palanisamy:** Data curation, Methodology, Software, Writing, Reviewing. **S. Usha:** Conceptualization, Validation, Writing – review & editing. **Mohit Bajaj:** Conceptualization, Validation, Writing – review & editing. **Hossam M. Zawbaa:** Resources, Writing – review & editing. **Salah Kamel:** Supervision, Writing – review & editing.

Declaration of competing interest

The authors declare that they have no known competing financial interests or personal relationships that could have appeared to influence the work reported in this paper.

Acknowledgments

The author (Hossam M. Zawbaa) thanks the European Union's Horizon 2020 research and Enterprise Ireland for their support under the Marie Skłodowska-Curie grant agreement No. 847402. The authors thank the support of the National Research and Development Agency of Chile (ANID), ANID/Fondap/15110019.

References

Al-Zamil, Torrey, D.A., 2000. Harmonic compensation for three-phase adjustable speed drives using active power line conditioner. USA, In: Power Engineering Society Summer Meeting, vol. 2, pp. 16–20.
Anon., 1993. IEEE Recommended Practices and Requirements for Harmonic Control in Electrical Power Systems. IEEE std., pp. 519–1992.

Arsov, L.j., Iljazi, I., Mircevski, S., Cundeva-Blajer, M., Abazi, A., 2012. Measurement of the influence of household power electronics on the power quality. In: 15th International Power Electronics and Motion Control Conference, EPE-PEMC 2012 ECCE Europe, Novi Sad, Serbia.
Baggini, Angelo, 2008. *Hand Book of Power Quality*. John Wiley and Sons Ltd, pp. 187–236.
Blazek, Vojtech, Petruzela, Michal, Vantuch, Tomas, Slanina, Zdenek, Mišák, Stanislav, Walendziuk, Wojciech, 2020. The estimation of the influence of household appliances on the power quality in a microgrid system. *Energies* 13, 4323. <http://dx.doi.org/10.3390/en13174323>.
Chen, J., Wang, W., Wang, S.H., Yang, S.M., 2016. An approach for electrical harmonic FFT analysis based on hanning self-multiply window. *Power Syst. Prot. Control* 19, 114–121.
Cho, Young-Sik, Cha, Hanju, 2011. A single-tuned passive harmonic filter design using transfer function approach for industrial process application. *Int. J. Mechatron. Autom.* 1 (2), 90–96.
Dao, T., Phung, B.T., Blackburn, T., 2015. Effect of Volage Harmonics on Distribution Transformer Losses, Power and Energy Engineering Conference. IEEE PES.
DaviCuriBusarello, Tiago, Pomilio, José Antenor, Simões, Marcelo Godoy, 2016. Passive filter aided by shunt compensators based on the conservative power theory. *IEEE Trans. Ind. Appl.* 52 (4), 3340–3347.
Diwan, Seema P., Inamdar, H.P., Vaidya, A.P., 2010. Simulation studies of shunt passive harmonic filters: six pulse rectifier load – Power factor improvement and harmonic control. In: Proc. of Int. Conf. on Advances in Electrical & Electronics, Sangli, India, pp. 205–210.
Dugan, Roger C., Mark, F., Mcgranaghan, Santos, Surya, Wayne Beaty, H., 2004. *Electrical Power Systems Quality*. The McGraw-Hill Companies.
Elphick, Sean, Ciufu, Phil, Drury, Gerrard, Smith, Vic, Perera, Sarath, Gosbell, Vic, 2017. Large scale proactive power-quality monitoring: An example from Australia. *IEEE Trans. Power Deliv.* 32 (2), 881–889.
Emanuel, A.E., Orr, J.A., Cyganski, D., Gulchenski, E.M., 1999. A survey of harmonics voltages, currents at the customer's bus. *IEEE Trans. Power Deliv.* 8, 411–421.
Farooq, Haroon, Zhou, Chengke, Allan, Malcolm, Farrag, Mohamed Emad, Khan, R.A., Junaid, M., 2011. Investigating the power quality of an electrical distribution system stressed by non-linear domestic appliances. In: International Conference on Renewable Energies and Power Quality ICREPQ'11, RE&PQJ, vol. 1, (9).
Gao, Z., Zhao, H., Zhou, X., Ma, Y., 2017. Summary of power system harmonics. In: 29th Chinese Control and Decision Conference CCDC, pp. 2287–2291.
Hamadi, Abdelhamid, Rahmani, Salem, Al-Haddad, Kamal, 2010. A hybrid passive filter configuration for VAR control and harmonic compensation. *IEEE Trans. Ind. Electron.* 57 (7), 2419–2434.
Jerin, Amalorpavaraj Rini Ann, Siano, Pierluigi, 2018. Smart grid and power quality issues. In: Hybrid-Renewable Energy Systems in Microgrids.
Karanki, K., Geddada, Nagesh, 2013. A modified three-phase four-wire UPQC topology with reduced DC-link voltage rating. *IEEE Trans. Ind. Electron.* 60 (9), 3555–3566.
Kavitha, V., Subramanian, K., 2017. Investigation of power quality issues and its solution for distributed power system. In: 2017 International Conference on circuits Power and Computing Technologies ICCPCT, 978-1-5090-4967.
Khalid, S., Dwivedi, Bharti, 2011. Power quality issues, problems, standards & their effects in industry with corrective means. *Int. J. Adv. Eng. Technol.* 1 (2), 1–11.
Kumar, Chandan, Mishra, Mahesh K., 2014. An improved hybrid DSTATCOM topology to compensate reactive and non-linear loads. *IEEE Trans. Ind. Electron.* 61 (2), 6517–6527.
Kumar, Dinesh, Zare, Firuz, 2014. Harmonic analysis of grid connected power electronic systems in low voltage distribution networks. *IEEE J. Emerg. Sel. Top. Power Electron.*
Malik, Hasmat, Iqbal, Atif, et al., 2021. Intelligent data analytics for power quality disturbance diagnosis using extreme learning machine (ELM). In: Intelligent Data-Analytics for Condition Monitoring.
Michaels, Kenneth M., 1997. Sensible approaches to diagnosing power quality problems. *IEEE Trans. Ind. Appl.* 33 (4), 1124–1130.
Mikkil, Suresh, Panda, Anup Kumar, 2015. Power quality issues and solutions-review. *Int. J. Emerg. Electr. Power Syst.* 16 (4), 175–181.
Niitsoo, Jaan, Taklaja, Paul, Palu, Ivo, Klüss, Joni, Power Quality Issues Concerning Photovoltaic Generation and Electrical Vehicle Loads in Distribution Grids.
Sahoo, Subrat, 2021. Recent trends and advances in power quality. In: *Power Quality in Modern Power Systems*.
Sangepu, Raghavendra, Vijay Muni, T., 2015. Effect of power quality issues in power system and its mitigation, power electronics devices. *Discovery* 28 (105), 72–79.

- Su, T.X., Yang, M.F., Jin, T., Flesch, R.C.C., 2018. Power harmonic and interharmonic detection method in renewable power based on Nuttall double-window all-phase FFT algorithm. *IET Renew. Power Gener.* 12, 953–961.
- Subjak, Joseph S., Jr., John, McQuilkin, S., 1998. Harmonics-causes, effects, measurements, and analysis: An update. *IEEE Trans. Ind. Appl.* 26 (6), 1034–1042.
- Swamy, Mahesh M., 2015. An electronically isolated 12-pulse autotransformer rectification scheme to improve input power factor and lower harmonic distortion in variable-frequency drives. *IEEE Trans. Ind. Appl.* 51 (5), 3986–3994.
- Toader, Cornel, Postolache, Petre, Golovanov, Nicolae, Porumb, Radu, Mircea, Ion, Mircea, Paul-Mihai, 2014. Power quality impact of energy-efficient electric domestic appliances. In: *International Conference on Applied and Theoretical Electricity ICATE*.
- Wagh, Karuna Nikum Abhay, Singh, Rakesh Saxena Arshita, 2019. Power quality problems in large commercial load and their mitigation: A case study. In: *2019 IEEE 1st International Conference on Energy, Systems and Information Processing, ICESIP, Chennai, India*, pp. 4–6.
- Wang, Guishuo, Wang, Xiaoli, Zhao, Chen, 2020. Iterative hybrid harmonics detection method based on discrete wavelet transform and Bartlett–Hann window. *Appl. Sci.* 10 (11), 3922. <http://dx.doi.org/10.3390/app10113922>.
- Yahya, Naderi, Guerrero, Josep M., et al., 2020. Power quality issues of smart microgrids: Applied techniques and decision making analysis. In: *Decision Making Applications in Modern Power Systems*.
- Zhong, Qing-Chang, Hornik, Tomas, 2013. Cascaded current–Voltage control to improve the power quality for a grid-connected inverter with a local load. *IEEE Trans. Ind. Electron.* 60 (4), 1344–1355.
- Zobaa, A.F., Abdel Aziz, M.M., Abdel Aleem, S.H.E., 2010. Comparison of shunt-passive and series passive filters for DC drive loads. *Electr. Power Compon. Syst.* 38 (3), 275–291.